

Evaluation of the Microstructure and Mechanical Properties of the Ultrafine Grained Thin-Walled Tubes Processed by Severe Plastic Deformation

H. Abdolvand¹, G. Faraji^{1,*}, M. K. Besharati Givi¹, R. Hashemi², and M. Riazat¹

¹School of Mechanical Engineering, College of Engineering, University of Tehran, Tehran, 11155-4563, Iran.

²School of Mechanical Engineering, Iran University of Science and Technology, Tehran, Iran.

(received date: 21 May 2015 / accepted date: 31 July 2015)

In this paper, ultrafine-grained (UFG) Cu-Zn tubes were processed via multi-pass parallel tubular channel angular pressing (PTCAP) process, and microstructure, mechanical properties along the axial and peripheral directions were evaluated. Mechanical characterizations were done using uniaxial tension test along both the axial and peripheral directions and biaxial bulging tests. The hydro-bulging test was used to measure the bursting pressure of UFG tubes. The results present that the UFG and nanostructured tubes achieved form PTCAP process exhibit excellent pressure bearing capacity in comparison with the coarse-grained (CG) counterparts. Also, the bursting pressure of the UFG tube was remarkably increased to 93 MPa just after the first pass of PTCAP process from 43.3 MPa for the CG one. It was 88 MPa and 81.3 MPa for second and third passes PTCAP processed tube. Important reasons for this behavior were both significant grain refinement and severe mechanical anisotropy results from texture evolution after PTCAP processing.

Keywords: nanostructured materials, severe plastic deformation, grain refinement, mechanical properties, microstructure

1. INTRODUCTION

Cylindrical tubes are common structural components employed in different industries. So, the burst pressure evaluation is an important consideration in the design for reliability, and it has been the subject of some researchers. In the last decades, the technology of tube hydroforming has aroused much attention for industrial applications. It allows reducing the number of welding spots and achieving complicated hollow shaped parts with the higher quality [1-4]. Several forming factors influence to tube hydroforming process. Among these factors, the material property plays a significant role in the magnitude of internal pressure, loading path, thickness distribution and die filling [5,6]. Hydroforming process is a relatively new technology as compared to other conventional forming processes. So, there is a little mechanical data for the material used in the hydroforming process, especially for UFG and nanostructured materials. The hydro-bulging test has been accepted as an appropriate method to examine the bursting pressure and the mechanical properties of the tubular shaped materials. It is an applicable method to determine a biaxial stress-strain relationships [7]. The hydro-bulging test seems to be a proper method to evaluate the effect of grain size on bursting pressure and bulge height of UFG tubes.

The UFG tube materials are produced by severe plastic deformation (SPD) techniques. The objective of the SPD processes is to provide high strength to weight materials, without any substantial dimensional change of workpiece [8]. Tubular channel angular pressing (TCAP) [9], tube cyclic extrusion compression (TCEC) [10], and high pressure tube twisting (HPTT) [11] were proposed as SPD methods suitable for tubular materials. Parallel tubular channel angular pressing (PTCAP) method developed by Faraji *et al.* gives better stain homogeneity and lower processing force in comparison with other processes [12]. The PTCAP process consists of two half cycles shown schematically in Fig. 1. The first punch presses the tube material into the two shear zones (Fig. 1(a)) in the first half cycle. Then, in the second half cycles, the second punch presses it back to its initial dimensions (Fig. 1(b)). The equivalent strain achieved from the N passes of PTCAP process can be estimated via the following Eq. [12]:

$$\bar{\epsilon}_{PTCAP} = 2N \left\{ \sum_{i=1}^2 \left[\frac{2 \cot(\phi_i/2 + \psi_i/2) + \psi_i \operatorname{cosec}(\phi_i/2 + \psi_i/2)}{\sqrt{3}} \right] + \frac{2}{\sqrt{3}} \ln \frac{R_2}{R_1} \right\} \quad (1)$$

where the parameters were shown in Fig. 1.

To predict the bursting pressure, Sevansson [13] proposed a formula and Xue *et al.* [14] modified it for thin-walled

*Corresponding author: ghfaraji@ut.ac.ir

tubes as follows:

$$P_b = \bar{\sigma}_u \left(\frac{0.25}{\bar{\varepsilon}_u + 0.227} \right) \left(\frac{2.718}{\bar{\varepsilon}_u} \right)^{\bar{\varepsilon}_u} \left(\frac{2t}{d} \right) \quad (2)$$

where P_b , $\bar{\varepsilon}_u$, $\bar{\sigma}_u$, t are d bursting pressure, equivalent ultimate strain, equivalent ultimate stress, thickness and mean diameter of the tube, respectively. By considering plane stress condition in biaxial deformation, equivalent stress and strain can be obtained from the following Eq. [15]:

$$\bar{\sigma} = \sqrt{(1 - \alpha + \alpha^2) \sigma_1} \quad (3)$$

$$\bar{\varepsilon} = \sqrt{\frac{4}{3}(1 + \beta + \beta^2) \varepsilon_1} \quad (4)$$

where $\alpha = 1/2$, and $\beta = 0$ in the hydro bulging test. Also, σ_1 and ε_1 are peripheral stress and strain, respectively.

In the present study, Cu-Zn brass tubes were processed by the PTCAP process through different cycles. Then, the bursting pressure of the UFG tubes under fluid pressure were investigated by hydro-bulging tests. The comparison of bursting pressures and maximum bulge heights between the annealed tube and the PTCAP processed UFG tubes were examined.

2. EXPERIMENTAL PROCEDURE

Cu-Zn (70/30 alloy) drawn brass tubular samples of 20 mm in outer diameter, 2.5 mm in thickness and 40 mm in length were annealed at the temperature of 600 °C for 1 h. A PTCAP die with the die parameters shown in Fig. 1(c), was manufactured. PTCAP process was applied to the tubes through one, two and three passes at a ram speed of 5 mm/min at room temperature while using molybdenum disulfide (MoS_2) as a lubricant. After each PTCAP process passes, an equivalent plastic strain of about 1.6 is applied. Tensile test samples were prepared in both axial and peripheral directions with gage length and width of 10 mm and 1 mm, respectively. A fixture for ring tensile test in the hoop direction is shown schematically in Fig. 2(b) [16]. Grease is used as a lubricant between split discs

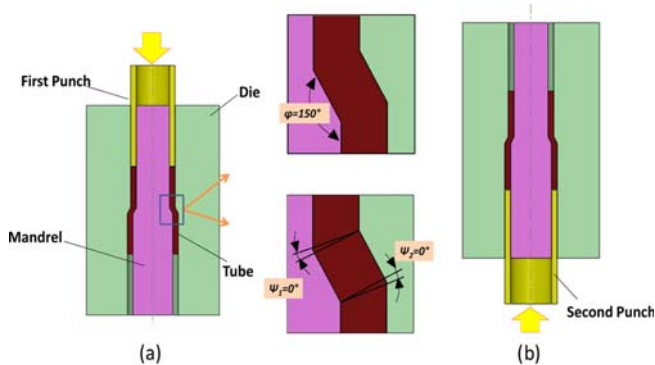


Fig. 1. Schematic of the PTCAP process; (a) the first and (b) the second half cycles.

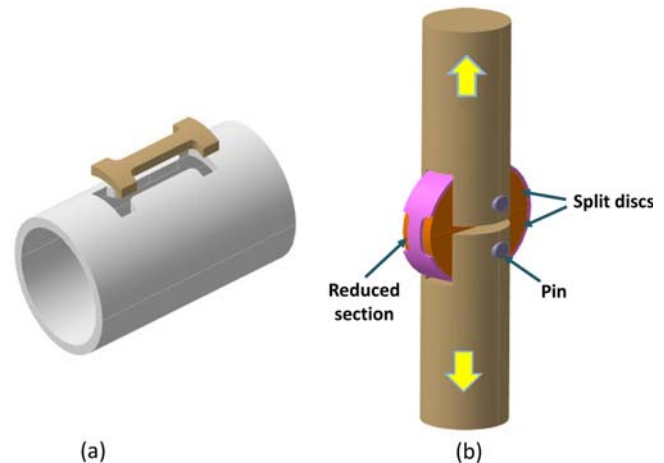


Fig. 2. (a) Schematic of tensile test location in the axial direction and (b) schematic of the ring hoop tensile test fixture.

and ring. All the tubes were machined to a length of 30 mm and thickness of 1 mm for the hydro-bulging test.

To implement the hydro-bulging test, a simple and the practical die, shown schematically in Fig. 3 was designed and manufactured. The main advantage of this tooling is that it needs no expensive and complicated hydraulic equipment, and high-pressure fluid could be achieved easily. The die was performed on a single-action press. After placing and locking the tube in the cavity between two supporting die using the urethane ring, the die is filled with hydraulic oil (Fig. 3). Then, the punch is pressed, and the fluid is pressurized. The internal pressure rises and makes the unsupported region of the tube bulge. The rising of the internal pressure continues until the tube bursts. The experiments were performed in a 300 kN Universal INSTRON press at a punch velocity of 2 mm/min. Fracture surface of the bursted tubes were analyzed using the scanning electron microscope (SEM).

3. RESULTS AND DISCUSSIONS

The optical microstructure of the annealed and PTCAP processed tubes can be observed in Fig. 4. Figure 4(a) shows fully recrystallized homogenous microstructure of the CG tube with an average grain size of about $\sim 70 \mu\text{m}$. As shown, the PTCAP process could significantly refine the microstructure. The microstructure changes during PTCAP process which is observed in Fig. 4(b-d). The shear zones exist in the PTCAP die, apply shear strain to the tube. During the SPD process, the shear deformation has a considerable effect on grain refinement, grain shape and texture [17]. After the first pass, the microstructure differs considerably from the annealed tube, and UFG structure is obtained (Fig. 4(b)). From Fig. 4 it is obvious that the higher accumulated strain results in finer grains. There is a saturation limit in refining the grain size. Faraji *et al.* reported that increasing the number of passes in

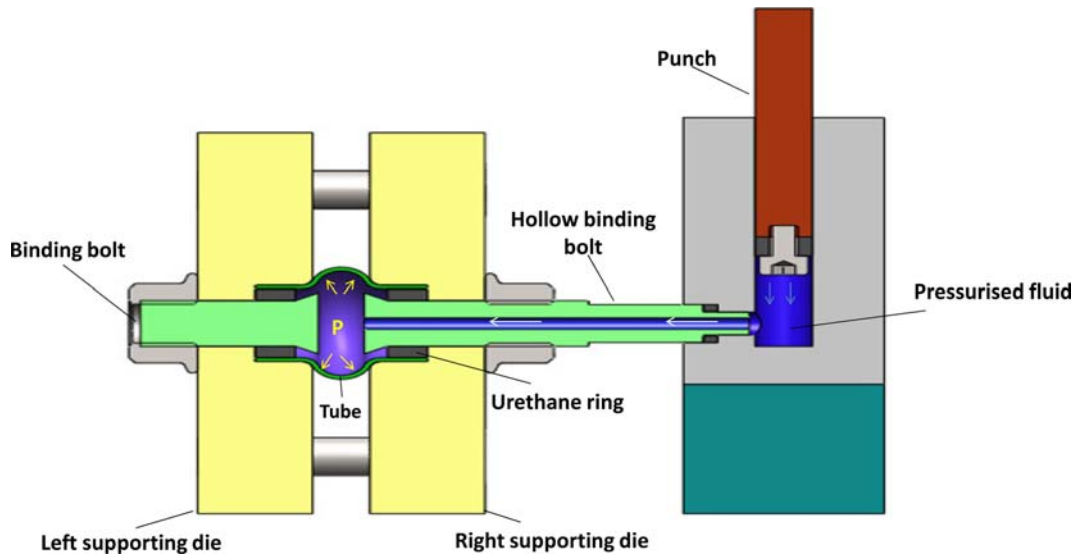


Fig. 3. Schematic of the tooling for the hydro-bulging test.

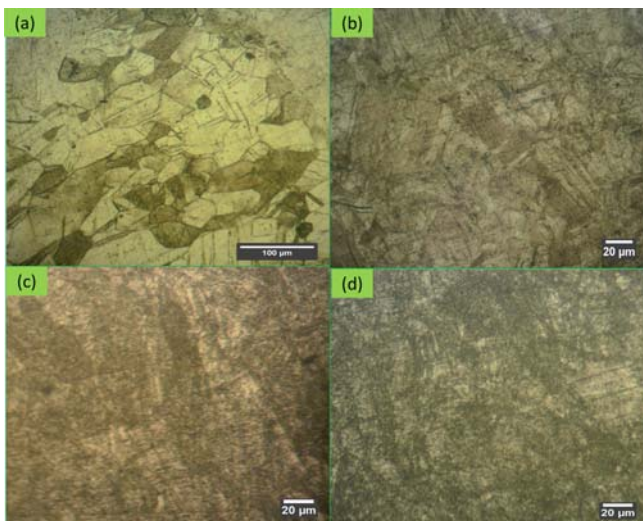


Fig. 4. Optical micrographs of (a) annealed tube and (b) first pass, (c) second passes, and (d) third passes PTCAP processed tubes.

PTCAP process on pure copper caused elongated grains were almost disappeared, and equiaxed grains were formed [18]. The same trend has been observed in other SPD methods [19-21].

Figure 5 exhibits variation of the ultimate strength and ultimate strain of the tubes through both axial and peripheral directions. It shows that imposing intense plastic strain results in enhancement of the strength and reduction at the elongation percent. The ultimate strength in axial and peripheral directions increased remarkably in one pass PTCAP processed tube about 62% and 102% respectively compared with those in annealed one. Though, the elongation to failure reduced almost 87% and 57%, respectively. This is an indication of the formation UFG structure and increased dislocation density. The well-known Hall-Petch equation proves that the grain

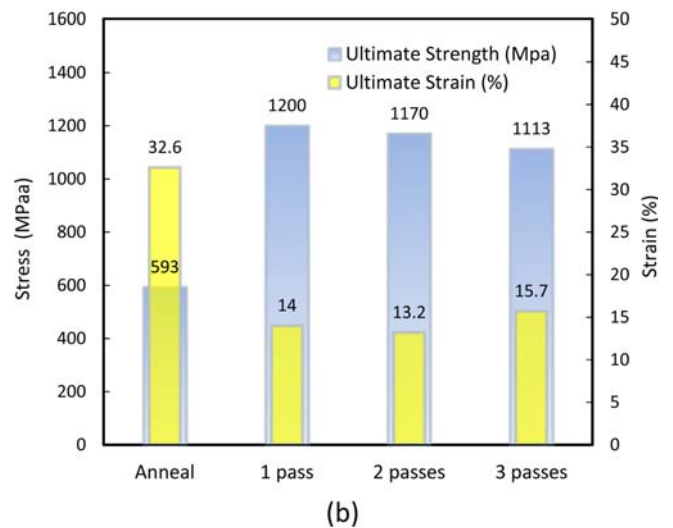
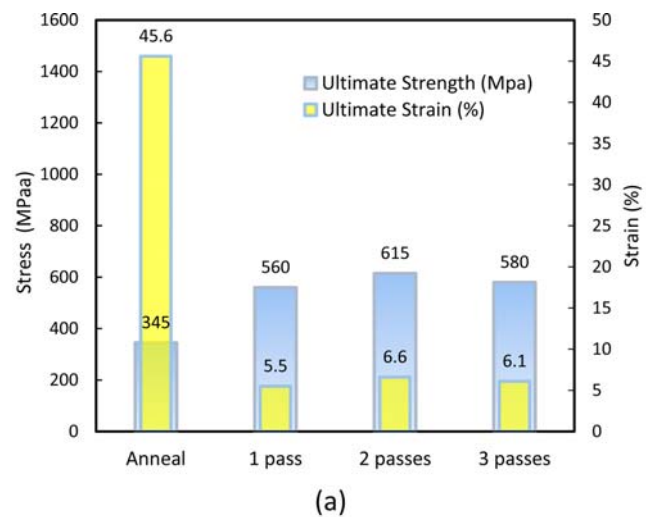


Fig. 5. Ultimate stress and ultimate strain variation of the samples in (a) axial direction and (b) peripheral direction.

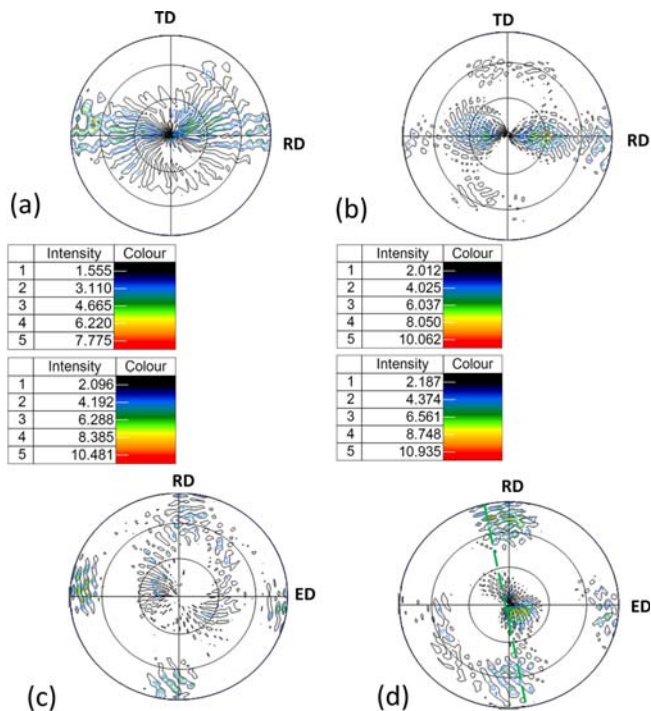


Fig. 6. $\{111\}$ pole figures of annealed and PTCAPed processed tubes in the axial direction ((a) and (b)), and peripheral direction ((c) and (d)), respectively. (ED: axial direction, RD: radial direction and TD is direction normal to the ED and RD directions) [22].

size plays a significant role on the mechanical properties of the materials. Reduction of the grain size impede the movement of dislocations [8]. As depicted, the ultimate strength in the peripheral direction increases more than the axial direction. Tavakkoli *et al.* [22] reported that it could be related to crystallographic texture of the brass tube changed during the PTCAP process which is shown in Fig. 6. It represents the texture of the tubes in two directions by X-ray diffraction technique. As shown, in the axial direction, orientation of the $\{111\}$ plane was unchanged after PTCAP process but intensity increased due to a generation of new grains by grain refinement (Fig. 6(b)) [23]. In peripheral direction after PTCAP process, the $\{111\}$ plane was rotated about 90° with reorientation toward the RD and the plane not exactly laid along the RD. This observation was the main cause of lower strength in axial direction compare to the peripheral direction. Better formability of the peripheral direction in comparison to the axial direction might be due to the different twinning behavior [24]. It is evident from Fig. 5 that most of the enhancement of the strength and reduction of the ductility have been obtained after only the first pass of PTCAP process and the second and third passes do not significantly changes the mechanical properties. This has been confirmed in other UFG metals, such as Ni, Ti and Al [25,26]. Meanwhile, the plasticity of the material was reduced.

Figure 7(a) shows the bulged and bursted CG, and PTCAP

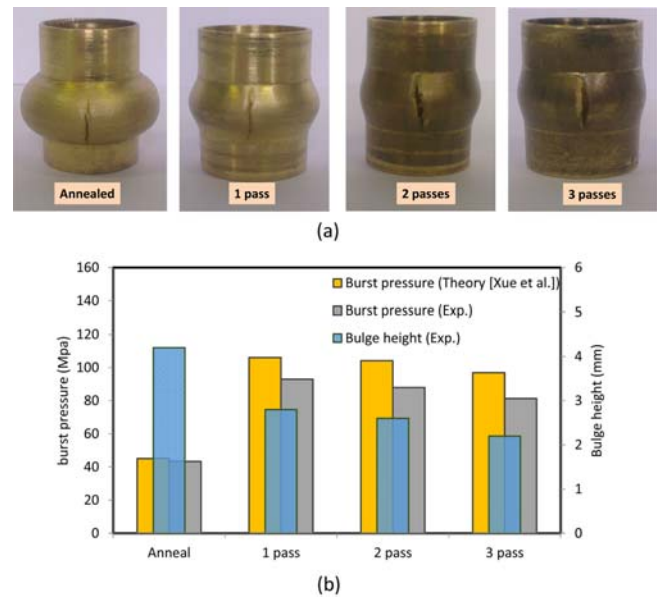


Fig. 7. (a) Annealed and PTCAP processed burst tubes after hydro-bulging test and (b) bursting pressures and bulged heights in the hydro-bulging test.

processed UFG tubes after the hydro-bulging test. Because of large hoop stresses in the peripheral direction, fracture always occurred parallel to the tube axis and thus the peripheral deformation is bigger than axial one. It should be noted that pressurizing rate is so effective and lower pressurizing rate leads to achieving more uniform strain distribution [27]. Precise comparison of the fractured areas demonstrates the substantial plasticity of the annealed tube while limited thinning in the PTCAP processed tubes. Figure 7(b) illustrates the variation of the bursting pressures and bulge heights in the CG and UFG samples. The bursting pressure of CG tube increased significantly from 43.3 MPa value to 93 MPa after the first pass of PTCAP process. In second and third passes PTCAP processed tubes, the bursting pressures decreased to 88 MPa and 81.3 MPa, respectively. In all UFG cases, the bursting pressure is significantly more than that of the CG tube. This variation of the bursting pressures are in agreement with the variation of the ultimate strength of the samples which were obtained from the tensile test. A high dislocation density and fine homogeneous grains which achieved after PTCAP process cause an increase in strength and results in a superior increase in the bursting pressure [12]. The bursting pressure of all samples is also calculated by Sevansson's formula, compared with experimental data and depicted in Fig. 7(b).

The calculated value of the annealed CG sample was about 45 MPa, which shows a small error of $\sim 4\%$ compared to the experiment. However, after the PTCAP process the error increased remarkably to 14%, 18% and 19% for the first, second, and third passes PTCAP processed tubes, respectively. The main reason may be related to severe mechanical anisotropy enhanced by PTCAP processing [22]. Other reasons could

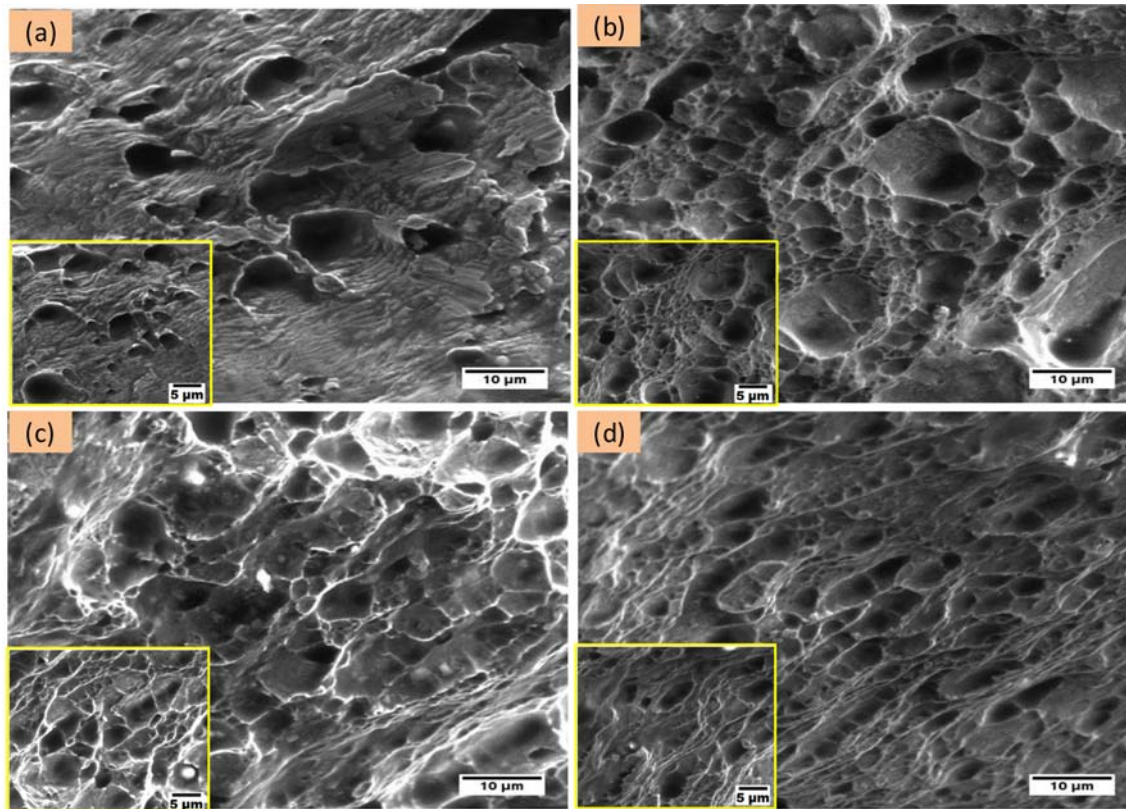


Fig. 8. SEM images showing the fracture surfaces of (a) CG annealed tube and (b) first pass, (c) second passes, and (d) third passes PTCAP processed tubes.

be non-uniform and eccentric loading or imperfect edge conditions of tubes [28].

As illustrated in Fig. 7(b), the bulged height of the samples reduced to 2.8 mm for the first pass PTCAP processed tube from 4.2 mm for the CG tube. Also, it was 2.6 mm and 2.2 mm for second and third passes processed tubes, respectively. So, it can be concluded that biaxial formability is also decreased. Higher slip systems are activated in biaxial tension state as compared to uniaxial one. So, a greater number of activated slip systems enable dislocations to form easily and uniform deformation to happen [29,30]. Recently, Tavakkoli *et al.* [22] reported that the PTCAP process makes a remarkable increase in ultimate strength. Also, increasing the strength of the brass tube in the peripheral direction is more than the axial direction. In the hydro-bulging test, a biaxial stress is applied to a tube in which higher strength exists in the peripheral direction. Thus, as the ultimate strength increases in the peripheral direction, it requires higher pressures to burst the tube.

SEM micrographs of the fractured surfaces of the bursted tubes were shown in Fig. 8. The shape, depth and direction of the dimples determine the type of the fracture. Annealed tube exhibited a typical ductile fracture because of the presence of deep, coarse and equiaxed dimples. By the increase in the internal pressure, the microvoids grow, propagate and coalescence, and finally cause failure. After PTCAP processing, small

dimples with varying size and shape with preferred orientations were observed (Fig. 8(b-d)). It is obvious that the annealed tube with bigger and deeper dimples exhibits a more formability than the PTCAP processed tubes. It is inconsistent with bulged height results shown in Fig. 7. For one pass PTCAPed sample as shown in Fig. 8(b) shallow and partly deep dimples oriented besides each other. For second and third passes PTCAPed tubes, the number of the shallow oriented dimples increased. The fracture mode changes from necking mode to shear mode after PTCAP process. Tavakoli *et al.* [22] showed that the UFG Cu-Zn tubes fractured by shear mode under tensile test along the peripheral direction. The number of the dimples were high, and the size of them were smaller than the dimples in the hydro-bulging test. It may be explained by the existence the biaxial deformation in which more strain can archive before failure. Thus, this process seems to be a useful method to evaluate the material property of the UFG tubes.

4. CONCLUSIONS

In this study, the biaxial free bulging behavior of the UFG tubes under hydro-bulging test was investigated for the first time. The effects of UFG microstructure on bursting pressure and bulge height of the brass tubes were examined. The

bursting pressure remarkably increased about ~114% after the first pass and ~103% and ~87% after second and third passes PTCAP processed UFG tubes, respectively. Also, the bulge height decreased from 4.2 mm for annealed tube to 2.8 mm for the first pass and 2.6 mm and 2.2 mm for second and third passes PTCAP processed tubes, respectively. Study of the fracture surface showed that the fracture mode changes from the necking mode in CG tube to shear mode in UFG tubes. The hydro-bulging test seems to be a proper method to evaluate the mechanical properties of the UFG tubes.

ACKNOWLEDGMENT

This work was financially supported by the Iran National Science Foundation (INSF).

REFERENCES

1. M. Ahmetoglu and T. Altan, *J. Mater. Process. Tech.* **98**, 25 (2000).
2. M. Koç and T. Altan, *J. Mater. Process. Tech.* **108**, 384 (2001).
3. L. H. Lang, Z. R. Wang, D. C. Kang, S. J. Yuan, S. H. Zhang, J. Danckert, and K. B. Nielsen, *J. Mater. Process. Tech.* **151**, 165 (2004).
4. B. J. Mac Donald and M. S. J. Hashmi, *J. Mater. Process. Tech.* **120**, 341 (2002).
5. Y. Aue-U-Lan, G. Ngaile, and T. Altan, *J. Mater. Process. Tech.* **146**, 137 (2004).
6. G. T. Kridli, L. Bao, P. K. Mallick, and Y. Tian, *J. Mater. Process. Tech.* **133**, 287 (2003).
7. M. Atkinson, *Int. J. Mech. Sci.* **39**, 761 (1997).
8. R. Z. Valiev, R. K. Islamgaliev, and I. V. Alexandrov, *Prog. Mater. Sci.* **45**, 103 (2000).
9. G. Faraji, M. M. Mashhadi, and H. S. Kim, *Mater. Lett.* **65**, 3009 (2011).
10. A. Babaei, M.M. Mashhadi, and H. Jafarzadeh, *Mat. Sci. Eng A-Struct.* **598**, 1 (2014).
11. L. S. Tóth, M. Arzaghi, J. J. Fundenberger, B. Beausir, O. Bouaziz, and R. Arruffat-Massion, *Scripta Mater.* **60**, 175 (2009).
12. G. Faraji, A. Babaei, M. M. Mashhadi, and K. Abrinia, *Mater. Lett.* **77**, 82 (2012).
13. N. Svensson, *J. Appl. Mech.* **25**, 89 (1958).
14. J. Hu, Z. Marciniak, and J. Duncan, *Mechanics of Sheet Metal Forming*, p.17, Butterworth-Heinemann, Oxford (2002).
15. J. Hu, Z. Marciniak, and J. Duncan, *Mechanics of Sheet Metal Forming*, Butterworth-Heinemann (2002).
16. Y.-L. Lin, Z.-B. He, S.-J. Yuan, and J. Wu, *T. Nonferr. Metal. Soc.* **21**, 851 (2011).
17. G. Faraji, M. M. Mashhadi, and H. S. Kim, *Mat. Sci. Eng A-Struct.* **528**, 4312 (2011).
18. G. Faraji, M. M. Mashhadi, A. R. Bushroa, and A. Babaei, *Mat. Sci. Eng A-Struct.* **563**, 193 (2013).
19. A. V. Nagasekhar, T. Rajkumar, D. Stephan, Y. Tick-Hon, R. K. Guduru, *Mat. Sci. Eng A-Struct.* **524**, 204 (2009).
20. S. Pasebani and M. R. Toroghinejad, *Mat. Sci. Eng A-Struct.* **527**, 491 (2010).
21. D. H. Shin, C. W. Seo, J. Kim, K.-T. Park, and W. Y. Choo, *Scripta Mater.* **42**, 695 (2000).
22. V. Tavakkoli, M. Afrasiab, G. Faraji, and M. M. Mashhadi, *Mat. Sci. Eng A-Struct.* **625**, 50 (2015).
23. W. J. Kim, C. W. An, Y. S. Kim, and S. I. Hong, *Scripta Mater.* **47**, 39 (2002).
24. L. Jiang, J.J. Jonas, K. Boyle, and P. Martin, *Mat. Sci. Eng A-Struct.* **492**, 68 (2008).
25. C. Gu, J. Lian, Z. Jiang, and Q. Jiang, *Scripta Mater.* **54**, 579 (2006).
26. F. Salimyanfard, M. R. Toroghinejad, F. Ashrafizadeh, and M. Jafari, *Mat. Sci. Eng A-Struct.* **528**, 5348 (2011).
27. M. Imaninejad, G. Subhash, and A. Loukus, *J. Mater. Process. Tech.* **147**, 247 (2004).
28. M. Koç and T. Altan, *International Journal of Machine Tools and Manufacture*, **42**, 123 (2002).
29. T. Minoda, K. Shibue, and H. Yoshida, *Journal-Japan Institute of Light Metals*, **54**, 110 (2004).
30. E. J. Pavlina, C. J. Van Tyne, and K. Hertel, *J. Mater. Process. Tech.* **201**, 242 (2008).